富山大学研究推進機構水素同位体科学研究センター研究報告35：13－22，2015.

論　文

Pt ナノ粒子の粒子成長と CO 吸着

田口 明*，尾崎 智弘

富山大学　研究推進機構　水素同位体科学研究センター

〒930-8555　富山市五福 3190

Growth and CO chemisorption study of platinum nanoparticles on α-Al_2O_3

Akira Taguchi*, Tomohiro Ozaki

Hydrogen Isotope Research Center

Organization for Promotion of Research, University of Toyama

Gofuku 3190, Toyama 930-8555

(Received January 28, 2016; accepted March 25, 2016)

Abstract

Pt nanoparticles sputter-deposited on α-Al_2O_3 support were investigated by FE-SEM measurements and CO chemisorption studies. Pt nanoparticles formed in the early stages of sputter deposition were well isolated, and the particle size distribution of Pt nanoparticles evaluated by FE-SEM measurements was narrow. Longer sputter deposition resulted in growth and coalescence of Pt nanoparticles. Such a transition of Pt from nanoparticles to film by sputter deposition was properly evaluated by CO chemisorption studies.

1. Introduction

Sputter deposition, a “dry” impregnation method that does not use any solvent or liquid for catalyst preparation, has gained attention because it has several advantages as compared to the conventional “wet” impregnation method. For example, dry processes enable efficient waste handling, which reduces the waste released to the environment. Further, sputter deposition from a source target allows the deposition of desired components on a substrate without impurities. Another advantage of using sputter deposition for catalyst preparation is that the nanoparticles are formed in appropriate conditions [1-5]. To achieve these principal benefits, novel sputter deposition systems for three-dimensional surfaces of powder substrates, rather than for conventional two-dimensional flat surfaces, have been developed by several research groups [6-15]. Au [11-13], VOx [14,15], Pt-Ru alloy [6,7,9] and Ru [8] were chosen as active species, and the catalysts obtained had certain intrinsic properties resulting from the dry impregnation method. For example, Veith et al. reported that Au/TiO_2 obtained by dc magnetron sputtering was structurally stable when heated to 500 ºC in air, whereas that obtained by the wet method was easily deactivated [13].

Among these publications [6,8,13] thermal treatment of sputter-deposited nanoparticles was used to control the particle diameter, although other research indicates that appropriate conditions for sputter deposition allows the control of the particle diameter of nanoparticles [5,10,16]. Here, we have investigated the growth of Pt nanoparticles on Al_2O_3 powder substrates as a function of the duration of sputter deposition. Change in the morphology of Pt nanoparticles were investigated by FE-SEM measurements. CO chemisorption studies were performed to estimate the Pt dispersion and Pt nanoparticle diameter.

2. Experimental

2.1. Preparation

The catalyst support, α-Al_2O_3, was kindly supplied by Sumitomo Chemical Co., Ltd., Tokyo (AA-18, surface area; 0.1−0.6 m^2/g in catalog). This was used after being dried overnight in an oven at 180 ºC. The metal plates (50 × 100 mm^2) used as a sputtering target were Pt (purity; 99.99 %).

Sputter deposition was conducted by using a barrel-sputtering system [6,10,17,18]. To the hexagonal barrel, 10.0 g of powdery α-Al_2O_3 was loaded in this study. A vacuum chamber equipped with the hexagonal barrel and powder substrate was evacuated to 8.0 × 10^{-4} Pa. High purity argon gas (99.995 %) was gradually introduced to the evacuated chamber up to 0.8 Pa, and this pressure was maintained during the sputter deposition. RF (13.56 MHz) magnetron sputtering was performed with an RF power of 25 W for an appropriate time (see Table 1), allowing Pt target to deposit on the surface of the catalyst supports. During the sputter deposition, about 4 times of back-and-forth (swinging) motion per 1 minute with ± 75º was applied to the hexagonal barrel to stir the powder substrates.

2.2. Characterization

Characterization of the obtained samples was carried out by using X-ray diffraction (XRD; Philips, PW1825/00), inductive coupling plasma analysis (ICP; PerkinElmer, Optima 3000XL) and field emission scanning electron microscopy (FE-SEM; JEOL, JSM-6701F). It should be noted that no further coating of the specimen, which is known to maintain the electron conductivity, was carried out in the FE-SEM measurements for samples.

The Pt dispersion of the prepared Pt/Al_2O_3 was measured by CO chemisorption method at atmospheric pressure. These studies were performed in a continuous flow reactor system with a quartz reactor (6 mm inner diameter). The Pt/Al_2O_3, typically loaded at 0.2–0.5 g, was heated to 250 ºC at a ramp rate of 5 ºC/min under He flow. At this temperature, fluid gas was changed to a mixture of H_2 (50 %) and He balance, and this temperature was

maintained for additional 1 h. After purging the gas to He, the catalyst in the reactor was cooled to room temperature. Then the catalyst bed was cooled to 0 ºC in an ice bath and maintained for 2 h. An appropriate amount (1 ml) of mixed gas of CO (0.5 %) and He balance was then injected into the catalyst in the reactor, and the concentration of CO in the outflow was detected by a thermal conductivity detector (TCD). The injection of CO was repeated until the amount of CO in the outflow became constant, where the CO adsorption was in saturation. The dispersion of Pt, hereafter denoted as D_{CO}, was calculated by assuming a 1:1 stoichiometry of CO:Pt, using the following equation:

$$D_{CO}=\frac{\text{number of CO molecule adsorbed}}{\text{number of Pt atom loaded}}$$

The above CO chemisorption was measured twice for each catalyst. The gas flow rate shown above was set to 30 ml/min.

3. Results

The amount of Pt deposited by various sputtering durations (4, 5, 7, 9 and 20 min) was evaluated by ICP measurements. The values were found to be 0.021, 0.032, 0.056, 0.075 and 0.136 wt%, respectively, as listed in Table 1. A linear correlation between the duration of sputter deposition and the amount of Pt was observed, which agreed with previous reports [6,10]. Hereafter, samples are denoted as Pt(x), where x represents the Pt deposition amount.

Table 1 Duration of sputter-deposition for preparation of Pt/Al_2O_3 and the summary of Pt particle diameter evaluated by FE-SEM measurements and CO chemisorption studies

Sample ID	Sputter-deposition time (min)	Pt deposition amount (wt%)	Pt diameter (FE-SEM) (nm)	CO chemisorption study		
				CO adsorbed (/g)	Pt dispersion (-)	Pt diameter (nm)
Pt(0.02)	4	0.021	1.8	2.18×10^{18}	0.70	1.7
Pt(0.03)	5	0.032	2.7	1.57×10^{18}	0.50	2.5
Pt(0.06)	7	0.056	3.9	0.95×10^{18}	0.31	4.5
Pt(0.08)	9	0.075	4.5	0.77×10^{18}	0.25	6.0
Pt(0.14)	20	0.136	5.1	0.57×10^{18}	0.18	8.2

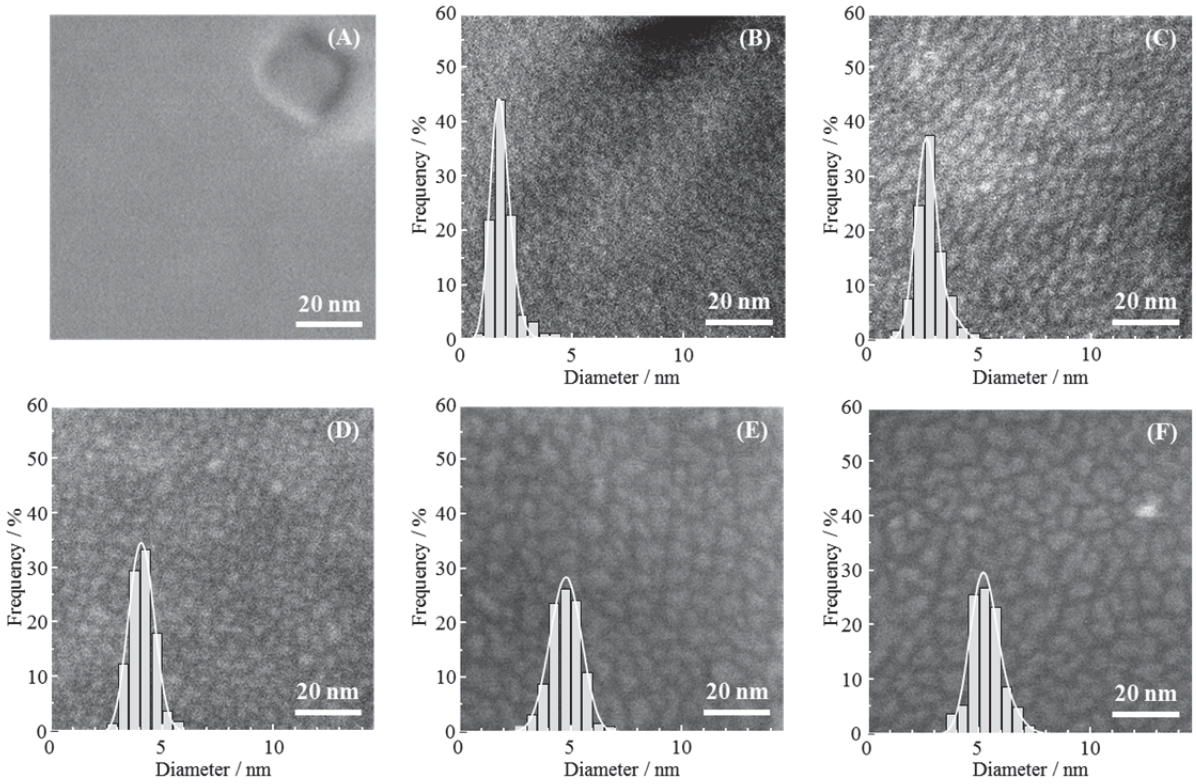

Fig. 1 FE-SEM images of the surface of the unmodified and Pt-modified samples. (A) unmodified Al_2O_3, (B) Pt(0.02), (C) Pt(0.03), (D) Pt(0.06), (E) Pt(0.08) and (F) Pt(0.14). The diagrams shown in (B)–(F) show the distributions of the size of Pt nanoparticles obtained from more than 200 nanoparticles.

The color of the sample was changed from white to gray by Pt deposition, and became continuously darker with the increase of Pt deposition. XRD measurement was attempted but diffraction signals from metallic Pt were not observed, even in the sample Pt(0.14), because the most of the diffraction lines from the Pt were overlapped by those from α-Al_2O_3.

Fig. 1 shows the FE-SEM images of unsupported Al_2O_3 and Pt/Al_2O_3. The surface of the unsupported Al_2O_3 is smooth (Fig. 1 (A)). A terrace-like structure seen in the upper right corner is an adhered fragment of Al_2O_3 that was used for focusing. The FE-SEM image of Pt(0.02) is shown in Fig. 1 (B), where Pt nanoparticles with circular shape are observed in the entire surface of the Pt/Al_2O_3. It was also found that the individual Pt nanoparticles were isolated on the Al_2O_3 surface. The distribution of the diameter of Pt nanoparticles, which was obtained from more than 200 nanoparticles, is overlaid in Fig. 1 (B).

The particle diameters ranged from 0.9 to 4.1 nm, and about 85 % of the Pt nanoparticles were in the range of 1.0–2.5 nm. The mean diameter, obtained from the peak in the Gram-Charlier fitting function (Origin 7.5 software; OriginLab Co., MA, USA), was calculated to be about 1.8 nm (Table 1). These findings indicate a good uniformity of the Pt nanoparticles on the powder substrate prepared by the barrel-sputtering technique.

In Pt(0.03), as shown in Fig. 1 (C), the mean diameter of Pt nanoparticles was determined to be 2.7 nm, which was larger than that of Pt(0.02). It was also found that the particle size distribution became wider (1.4–5.1 nm) than Pt(0.02). This indicates a growth of Pt nanoparticles with an increase in the duration of sputter deposition. However, it should be noted that each nanoparticle still maintained a circular shape, and was isolated. One interesting feature in dry impregnation, especially in the barrel-sputtering method, is that the Pt nanoparticles formed were free of facets [10]. This is consistent with data from typical two-dimensional sputter-deposition used for epitaxial film growth [19-21]. For example, Zhao and Wong reported that Pt deposited on a $SrTiO_3$(100) substrate under high temperature conditions (700 ºC) resulted in a highly crystalline Pt platelet film, whereas Pt deposition at a low temperature (25 ºC) resulted in an indistinct crystalline film [19].

In the sample of Pt(0.06), in Fig. 1 (D), a coalescence of Pt nanoparticles appeared to be started. The shape of the Pt nanoparticles was no longer circular: The Pt nanoparticles grew in size, with the result that some of the near neighbors came into contact to form irregular lengths and shapes. This resulted in the shifting and the widening the particle size distribution (2.1–5.9 nm), which was obtained in the elementary nanoparticles, as compared to Pt(0.03). The mean diameter of the Pt nanoparticles was 3.9 nm. These findings support to start the transition of Pt from nanoparticles to film. By long sputter deposition, the Pt nanoparticles grew in size, remarkably coalesced and formed worm-like structures which indicated a transition between isolated nanoparticles to film. In the sample Pt(0.08),

however, FE-SEM observation revealed that the coalescent particles in the worm-like structure consisted of several distinct elementary nanoparticles, as seen in Fig. 1 (E). The mean diameter of such elementary nanoparticles was estimated to be 4.5 nm. In addition, the distribution of the diameter of elementary nanoparticles became wider and shifted to larger values (2.6–6.6 nm) as compared to sample Pt(0.06). Such a growth and coalescence of Pt nanoparticles, in other words, the agglomeration of Pt nanoparticles was obvious in the case of Pt(0.14), as seen in Fig. 1 (F). The particle diameter ranged between 3.5 and 7.7 nm, and the mean particle diameter was about 5.1 nm.

CO chemisorption studies of unmodified α-Al_2O_3 showed no significant CO uptake (less than 2 % in the first injection). This suggests that CO molecules chemisorbed on Pt under these experimental conditions. The Pt dispersion obtained (D_{CO}) is listed in Table 1 and is plotted in Fig. 2 as a function of the mean particle diameter of Pt obtained from FE-SEM measurements. It can be clearly seen in Fig. 2 that the dispersion decreased drastically with an increase in particle diameter.

The changes in the idealized dispersion ($D_{cal.}$), which depends on the particle diameter, is also plotted in Fig. 2. Here, $D_{cal.}$ is calculated for a hemispherical crystallite of Pt particle as follows. From the unit cell parameter of metallic Pt (JCPDS 04-0802, a_0 = 0.39231 nm), the value of Pt atomic diameter, the number of Pt atoms per unit area in a closed-packed plane and that per unit volume in a closed-packed lattice (fcc) were found to be 0.277 nm, 15.01 atoms/nm^2 and 66.43 atoms/nm^3, respectively. The

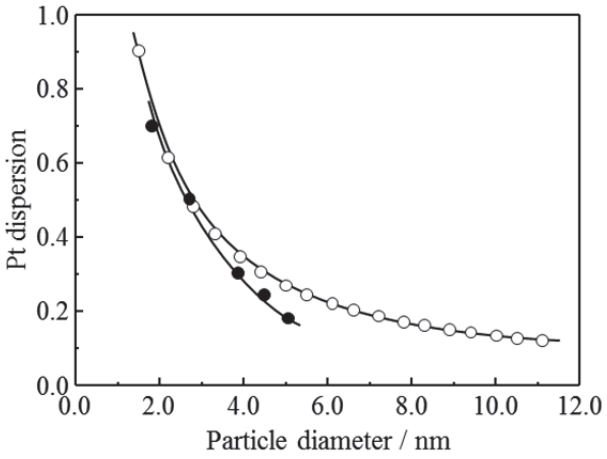

Fig. 2 Change in the dispersion of Pt nanoparticles as a function of particle diameter. (●) values obtained from CO chemisorption studies, (○) theoretical values calculated from the hemispherical crystallites.

number of Pt atoms on the nanoparticle surface ($Pt_{surface}$) and that in the whole nanoparticle ($Pt_{particle}$) can be represented as follows:

$$Pt_{surface} = \frac{1}{2}\pi d^2 \times 15.01$$

$$Pt_{particle} = \frac{1}{12}\pi d^3 \times 66.43$$

Here, d represents the diameter of the Pt nanoparticle. Thus, $D_{cal.}$ can be expressed as follows:

$$D_{cal.} = \frac{Pt_{surface}}{Pt_{particle}}$$

For particle diameters smaller than about 3.0 nm (Fig. 2), it is found that the value of D_{CO} agrees well with that of D_{cal}. This means that the results from FE-SEM observation appropriately capture the Pt dispersion. On the other hand, the value of D_{CO} becomes smaller than that of D_{cal}. When particle diameters are greater than about 3.0 nm (Fig. 2). The divergence in the case of large particles is mainly attributed to coalescences of the Pt nanoparticles because the D_{CO} with agglomerated nanoparticles can easily cause the underestimation of particle diameter. The FE-SEM observations described above also support the coalescence of Pt nanoparticles with diameters greater than 3.0 nm, which corresponds to Pt(0.06).

4. Conclusions

A novel “dry” impregnation method, named the barrel-sputtering method, was applied to prepare α-Al_2O_3 supported Pt catalysts. Isolated Pt nanoparticles with a mean diameter of 1.8 to 2.7 nm were observed by FE-SEM measurements of a sample of relatively short duration of sputter-deposition. CO chemisorption studies revealed that Pt dispersion was 0.70 and 0.50, respectively. These values were in good agreement with the ones calculated geometrically from the particle diameters. These findings indicate that the barrel-sputtering

method can fabricate isolated Pt nanoparticles. Further, it suggests that the dispersion was appropriately estimated on the basis of FE-SEM measurements when the nanoparticles were well isolated. Moreover, longer sputter-deposition led to growth and coalescence of Pt nanoparticles, which were clearly observed by FE-SEM. CO chemisorption studies also supported the agglomeration of Pt nanoparticles.

References

[1] V. Meille, Appl. Catal. A: Gen. 315 (2006) 1.
[2] A.-L. Thomann, J. P. Rosenbaum, P. Brault, C. Andreazza, P. Andreazza, B. Rousseau, H. Estrade-Szwarckopf, A. Berthet, J. C. Bertolini, F. J. Cadete Santos Aires, F. Monnet, C. Mirodatos, C. Charles, R. Boswell, Pure Appl. Chem. 74 (2002) 471.
[3] S. C. Tjong, H. Chen, Mater. Sci. Engineer. R45 (2004) 1.
[4] F. H. Kaatz, G. M. Chow, A. S. Edelstein, J. Mater. Res. 8 (1993) 995.
[5] P. Brault, A.-L. Thomann, C. Andreazza-Vignolle, P. Andreazza, Eur. Phys. J. AP 19 (2002) 83.
[6] M. Inoue, H. Shingen, T. Kitami, S. Akamaru, A. Taguchi, Y. Kawamoto, A. Tada, K. Ohtawa, K. Ohba, M. Matsuyama, K. Watanabe, I. Tsubone, T. Abe, J. Phys. Chem. C 112 (2008) 1479.
[7] M. Inoue, S. Akamaru, A. Taguchi, T. Abe, Vacuum 83 (2009) 658.
[8] T. Abe, M. Tanizawa, K. Watanabe, A. Taguchi, Ener. Environment. Sci. 2 (2009) 315.
[9] M. Inoue, T. Nishimura, S. Akamaru, A. Taguchi, M. Umeda, T. Abe, Electrochim. Acta 54 (2009) 4764.
[10] A. Taguchi, M. Inoue, C. Hiromi, M. Tanizawa, T. Kitami, T. Abe, Vacuum 83 (2009) 575.
[11] G. M. Veith, A. R. Lupini, S. J. Pennycook, G. W. Ownby, N. J. Dudney, J. Catal. 231 (2005) 151.
[12] G. M. Veith, A. R. Lupini, S. J. Pennycook, A. Villa, L. Prati, N. J. Dudney, Catal. Today 122 (2007) 248.
[13] G. M. Veith, A. R. Lupini, S. Rashkeev, S. J. Pennycook, D. R. Mullins, V. Schwartz, C. A. Bridges, N. J. Dudney, J. Catal. 262 (2009) 92.
[14] H. Poelman, B. F. Sels, M. Olea, K. Eufinger, J. S. Paul, B. Moens, I. Sack, V. Balcaen, F. Bertinchamps, E. M. Gaigneaux, P. A. Jacobs, G. B. Marin, D. Poelman, R. De Gryse, J. Cata. 245 (2007) 156.
[15] H. Poelman, K. Eufinger, D. Depla, D. Poelman, R. De Gryse, B. F. Sels, G. B. Marin, Appl. Catal. A: Gen. 325 (2007) 213.

[16] L. Armelao, D. Barreca, G. Bottaro, G. Bruno, A. Gasparotto, M. Losurdo, E. Tondello, Mater. Sci. Engineer. C 25 (2005) 599.
[17] T. Abe, S. Akamaru, K. Watanabe, J. Alloys Compd, 377 (2004) 194.
[18] T. Abe, S. Akamaru, K. Watanabe, Y. Honda, J. Alloys Compd. 402 (2005) 227.
[19] K. Zhao, H. K. Wong, J. Cryst. Growth 256 (2003) 283.
[20] C. Gate., P. Baules, E. Snoeck, J. Cryst. Growth 252 (2003) 424.
[21] C. Gatel, E. Snoeck, Surf. Sci. 600 (2006) 2650.